JOURNAL OF SCIENCE, TECHNOLOGY AND ENGINEERING RESEARCH
*Bilim, Teknoloji ve Mühendislik Araştırmaları Dergisi*
ISSN (Online) 2717-8404
Available *online* at https://dergipark.org.tr/en/pub/jster

RESEARCH ARTICLE

# Impedance Controller Design and Dynamic Solution of The Manipulandum

[*]Yaşar Yıldıran, [1]Babek Naseri, [2]Amir Nobahar and [3]Reşat Özgür Doruk

[*]Atılım University, Graduate School of Natural and Applied Sciences, Department of MODES, Ankara, Türkiye
yasaryildiran@gmail.com, Orcid.0009-0003-2963-9203
[1]Atılım University, School of Engineering, Mechatronics Engineering Department, Ankara, Türkiye
babek.naseri@atilim.edu.tr, Orcid.0000-0001-6007-3875
[2]Atılım University, School of Engineering, Mechatronics Engineering Department, Ankara, Türkiye
amir.nsnam@atilim.edu.tr, Orcid.0000-0002-8248-4963
[3]Atılım University, School of Engineering, Electrical-Electronics Engineering Department, Ankara, Türkiye
resat.doruk@atilim.edu.tr, Orcid.0000-0002-9217-0845

**Citation:**
Yıldıran, Y., Naseri, B., Nobahar, A., Doruk, R.Ö. (2024). *Impedance Controller Design and Dynamic Solution of The Manipulandum*, Journal of Science, Technology and Engineering Research, 5(1):54-67. DOI: 10.53525/jster.1475764

**Article Info**

*Received : 30 April 2024*
*Accepted : 28 May 2024*

**DOI:**
10.53525/jster.1475764

***Corresponding Author:**
Yaşar Yıldıran
yasaryildiran@gmail.com
Phone: +90 533 634 0330

**ABSTRACT**

*This article explains the dynamic solution of the manipulandum that interact with the human upper arm, controller design, model simulation and simulation results. Manipulandum design are used in human-machine interaction experiments to understand human motor learning skills. Experimental design is the subject of the field of medicine, appropriate manipulandum design is the subject of the engineering field. In this article, the engineering qualities of the device were evaluated, its mathematical model obtained, dynamic model simulation made and control elements were examined, but the experimental use of this device, which is serve medical science were not discussed in this context. Most manipulandum in the literature have a 2-dof, 5-link closed chain structure that moves in the horizontal plane, their movement is provided by 2 actuators, their interaction with the human upper arm is made with a fixed joystick (end-effector) on the 2nd link, and their dimensions are smooth and compatible with the human upper arm. It is understood that the manipulandum must be of a size that can safely interact with the human arm. In this study a conceptual design was made for the manipulandum and the movement parameters of the manipulandum were obtained by creating a kinematic model accordingly. While creating the dynamic model of the system; It is accepted that the manipulandum moves in the horizontal plane, therefore there is no effect of gravity, there is no spring, damper or similar potential energy source in the system, and there is heat loss due to friction. The dynamic model obtained with the Euler Lagrange Method (ELM) was compared with the system model obtained with the Simulink Simscape Multibody (SSM) tool in the Simulink environment; The consistency of model parameters (friction coefficients, moment of inertia, etc.) was mutually checked. Since human-manipulandum interaction requires force control, an impedance controller has been designed for the system dynamics, instead of classical controllers. The success of the controller on both the ELM dynamic model and the SSM dynamic model were examined and the results were evaluated. As a result of the simulations; It is understood that in order to achieve meaningful position and force control, there must be a proportional magnitude relationship between the torques applied to the model by the actuators and the force applied to the end-effector.*

**Keywords:** *Manipulandum, Haptic Device, System Dynamics, Impedance Controller*

## I. INTRODUCTION

Motor behavior examines the ability to perform the movement at the optimum level. Motor learning is defined as the acquisition of motor skills and permanent improvement in performance. To master or adapt to a motor skill, a behavior must be repeated over and over. Today, robotic manipulandum's are frequently used in applied experiments to understand motor learning. Robotic manipulandum's are in a structure that moves in a planar surface, in a close chain structure, interacting with the subject via a joystick at the end-effector.
Manipulandum produce physical feedback to user. Their interface has to be ensured with physical interaction. With this properties manipulandum, they are preferable as robotic training devices for upper limb training for stroke rehabilitation. Compared to conventional therapies, these training devices have the advantage that they allow a self-controlled increase in training intensity and frequency as well as the opportunity to train independently [1].

In the literature Howard et al. used the vBOT planar robotic manipulandum to investigate whether the actions performed are independent of the last state in motor memory [2]. Again Howard et al.; used vBOT to investigate the effects of lead-in movement on motor memory formation. In their experiments, they observed that the active lead-in movement provided by vBOT reduced motor adaptation [3]. In their article Gomi and Kawato discussed a method aimed at measuring upper arm stiffness during movement. For this purpose, they developed a manipulandum in parallel link structure that can test both arms at the same time [4]. Kinarm End-Point is a commercial manipulandum used by clinical researchers to understand the effects of various neurological injuries and diseases. The Kinarm End-Point manipulandum is a stiff, graspable robot that can create highly complex mechanical environments [5]. With these features, it allows researchers to collect large amounts of valuable data in understanding brain functions and nervous system in studies conducted with healthy individuals. More than 200 publications have been made in this field using Kinarm End-Point [5]. Klein et al. described the 3-dof redundant motor control interface, its design features and the experimental results on a subject in their publications. Manipulandum also has an unusual wrist motor [6]. In the publications of Kostic and Popovic; a manipulandum without an actuator that moved freely in the horizontal plane was used. During the experiment, data was collected through the trace of the magnetic mouse attached to the End-effector on the Wacom Intuos4 plane. The subject's point to point movement was evaluated [7]. In their publication, Fong et al. designed a manipulandum with transparency and gravity compensation features to be used in upper-limp rehabilitation [8]. In their publications, Ueyama and Miyashita used a manipulandum called RANARM to estimate the limp stiffness of the monkey they chose as a subject [9]. In their publication, Cai and colleagues shared the features and first experiment of the dual-arm manipulandum they developed for use in the physical therapy of stroke patients. Dual-Arm Rehabilitation Robot (DARR) is designed to work synchronously with two 3-dof robotic arms attached to the subject's arm, one on the upper arm and the other on the lower arm [10]. Khanh Tran Nguyen and Hoang Dung Nguyen shared the features of the 1 dof dual manipulandum, which they designed to be used in the physical therapy of post-stroke patients, in their publications [11]. In their publications, Asgari and Crouch created a simulation model to estimate human upper arm impedance. The success of the study is the physical interaction with both the manipulandum model and the human model created through OpenSim in the simulation environment [12]. Vlugt et al. studied the mechanical properties of the human arm, which acts in harmony with a haptic device. Their 2003 article describe the design and application of the haptic device. They predicted that the deviation in position could be recorded as a result of the irregularity in the force, thus estimating the human endpoint admittance [13].

Literature shows that engineering and medical sciences are in a solid relationship in the design and use of manipulandum. Manipulandum have two main uses. The first is to investigate motor learning skills on healthy individuals, and the other is to use it as an auxiliary tool in the physical therapy of disabled individuals. With this study, it is aimed to complete the engineering design of a concept manipulandum that will serve to investigate motor learning skills on healthy individuals. First, a concept model of a manipulandum that will interact with the human upper arm is designed in the scope of the article. The study also includes obtaining the mathematical model (kinematic and dynamic model) for the two-axis five-bar

manipulandum, selecting and designing the controller, simulating the success of the controllers, and evaluating the simulation results.

## II. MATERIALS AND METHODS

### II.1. KINEMATIC MODEL

First of all, the notations of the two DOF five-bar planar manipulandum mechanism should be defined. Figure-1 shows the kinematic parameters on the manipulandum concept design. Manipulandum consists of five links, one fixed frame and four movable links, and five revolute joints connecting these links. $L_i$ moving link lengths (in meters) as i=1,2,3,4,5, $\theta_i$ represent the angles (in radians) of the links counterclockwise with the X-axis. Links $L_1$ and $L_2$ are connected to the fixed frame by two overlapping revolute joints at $X_0$, $Y_0$ coordinates. The angular changes in $L_1$ and $L_2$ are both measured counterclockwise with respect to the X-axis and are defined by $\theta_1$ and $\theta_2$, respectively. These two revolute joints are the active revolute joints of the system. $L_3$-$L_1$ and $L_4$-$L_2$ links are connected to each other by passive revolute joints and the angular change in these two passive revolute joints are defined by $\theta_3$ and $\theta_4$, respectively. The closed chain structure of the manipulandum, the overlap of the $L_1$ and $L_2$ links at the $X_0$, $Y_0$ point, the selection of the $L_1$-$L_4$ and $L_2$-$L_3$ links of equal length, allows the structure to turn into a parallelogram, which provides an easy solution of the mathematical model. The $L_5$ link is fixedly connected to the $L_4$ link in the same direction, and it is connected to the $L_3$ link with a passive revolute joint. The kinematic model of the system drive according to these parameters.

Manipulandum motion states (position, velocity, acceleration) are obtained by constructing the kinematic model. Kinematic model must accurately represent every position and movement within the working area of the manipulandum. The expectation from the Manipulandum kinematic model is that it provides the relationship between $\theta_1$ and $\theta_2$ entry angles and the end-effector cartesian coordinates.

$L_1$ and $L_2$ are active links and their motions are independent. Therefore, the end-effector position equations from both branches should be written separately. However, due to choosing $L_3$ and $L_4$ link lengths as $L_3$=$L_2$ and $L_4$=$L_1$, $\theta_3$ angle is equal $\theta_2$ (in radians) and $\theta_4$ angle is equal $\theta_1$ angle (in radians), respectively. In future formulations, the equivalents of $L_3$, $L_4$, $\theta_3$ and $\theta_4$ will be used instead.

$$x = (L_1 + L_5).cos\theta_1 + L_2.\cos\theta_2 \quad (1)$$

$$y = (L_1 + L_5).sin\theta_1 + L_2.sin\theta_2 \quad (2)$$

For real-time control of the manipulandum, it is also necessary to obtain the inverse kinematics equations. Craig gives some inverse kinematic solutions in chapter 4 of Introduction to Robotics Mechanics and Control book [14]. The sum of the squares of equations (1) and (2) is the equation (3).

$$x.\cos\theta_2 + y.\sin\theta_2 = \frac{(x^2+y^2)+{L_2}^2-(L_1+L_5)^2}{2.L_2} \quad (3)$$

Craig suggested that at appendix C that, if equation (3) is transcendental form and right-hand side is constant, inverse kinematic solution for $\theta_2$ will be equation (4).

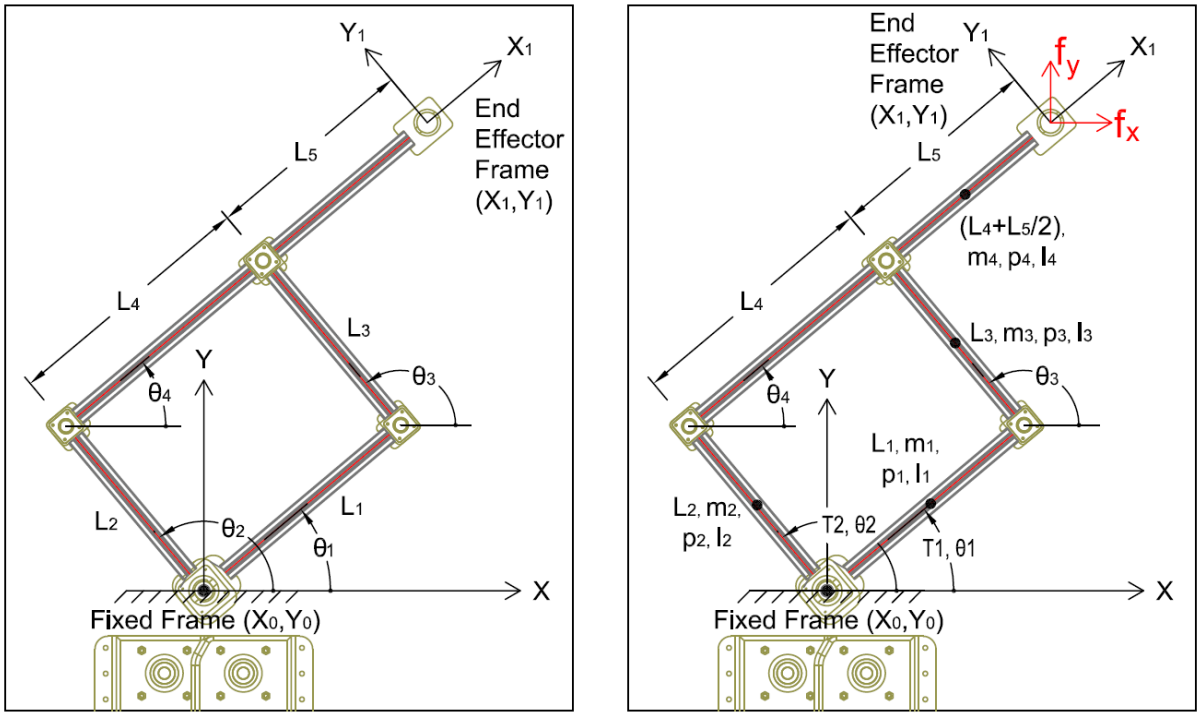


**Figure. 1.(a)** Two-DOF Five-bar Planar Manipulandum Kinematic Parameters, **Figure. 1.(b)** Two-DOF Five-bar Planar Manipulandum Dynamic Parameters.

$$\theta_2 = \arctan\frac{y}{x} \pm \arctan\left(\frac{\sqrt{x^2+y^2-\left(\frac{(x^2+y^2)+{L_2}^2-(L_1+L_5)^2}{2.L_2}\right)^2}}{\frac{(x^2+y^2)+{L_2}^2-(L_1+L_5)^2}{2.L_2}}\right) \qquad (4)$$

Similarly, if $cos\theta_1$ is let alone from equation (1), inverse kinematic solution for $\theta_1$ will be equation (5).

$$\theta_1 = \arctan\left(\pm\frac{\left(\frac{x-L_2.\cos\theta_2}{(L_1+L_5)}\right)}{\sqrt{1-\left(\frac{x-L_2.\cos\theta_2}{(L_1+L_5)}\right)^2}}\right) \qquad (5)$$

So, system forward and inverse kinematics models are defined mathematically. With this way end-effector XY position can be describe according to $\theta_2$ and $\theta_1$. Jacobian Matrix provides the relation between joint velocities & end-effector velocities of manipulandum. It can be obtained from equations (1) and (2).

$$\begin{bmatrix} x' \\ y' \end{bmatrix} = \begin{bmatrix} -(L_1+L_5).sin(\theta_1) & -L_2.sin(\theta_2) \\ (L_1+L_5).cos(\theta_1) & L_2.cos(\theta_2) \end{bmatrix} \begin{bmatrix} \theta_1' \\ \theta_2' \end{bmatrix} = J.\theta' \qquad (6)$$

### II.2. DYNAMICAL MODEL

The joint space dynamics of the human interacting manipulandum is defined by equation (7).

$$M(\theta).\theta" + V(\theta,\theta') + g(\theta) = \tau + J(\theta)^T f \qquad (7)$$

Here, $M(\theta).\theta"$, $V(\theta,\theta')$ and $g(\theta)$ are the inertial matrix, centrifugal and coriolis forces, and the gravitational component, respectively. The position of the manipulandum in the joint space is defined by $\theta = [\theta_1;\theta_2]$, the actuator torque (N.m) vector is defined by $\tau = [\tau_1;\tau_2]$, the manipulandum Jacobian is defined by $J(\theta)$, and the force vector is defined by $f = [f_x;f_y]$, which is applied force (N) externally to the

end-effector. Since the manipulandum working area is a two-dimensional horizontal plane, the effect of gravity is neglected. Here $f$ is the force, so modeling of the interacting human upper arm was not required, as it was measured by sensors in the joystick-shaped end-effector [15],[16],[17].

While creating the dynamic model of Manipulandum, the Euler-Lagrange method (ELM) was used. Energy components of the system; Kinetic energy T, dissipating energy D and potential energy U must be known. Since the Manipulandum has no movement on the vertical axis and there is no spring or similar element in the system to store energy, potential energy change in the system is assumed to be zero. It is accepted that the source of dissipating energy is the friction occurring at the joints and end-effector. For each link, the energy lost in the joints was calculated as ($D_i = \frac{1}{2}.C_i.(\theta_i' - \theta_{i-1}')^2$), thus the total dissipating energy "D" was obtained. The derivative of the dissipating energy affecting the system is calculated for the joints, where "$C_i$" is the friction coefficient it is given by equations (8) and (9).

$$\frac{\partial D}{\partial \theta_1'} = (C_1 + C_3 + C_4).\theta_1' + (C_4 - C_3).\theta_2' \quad (8)$$

$$\frac{\partial D}{\partial \theta_2'} = (C_2 + C_3 + C_4).\theta_2' + (C_4 - C_3).\theta_1' \quad (9)$$

The parameters used when calculating the kinetic energy "$T_i$" of the system are; "$L_i$" as the link length, "$m_i$" as the link mass, "$v_i$" as the center of mass linear velocity component, "$p_i$" as the center of mass position, and "$I_i$" as the link moment of inertia. Here "$p_4$" is the center of mass that is assumed as the center of mass of the total mass of the "$L_1$", "$L_5$" links and the end-effector. The kinetic energy equation for each component are given by (10), (11), (12), and (13).

$$T_1 = \frac{1}{2}.m_1.v_1^2 + \frac{1}{2}.I_1.\theta_1'^2 \quad (10) \qquad T_2 = \frac{1}{2}.m_2.v_2^2 + \frac{1}{2}.I_2.\theta_2'^2 \quad (11)$$

$$T_3 = \frac{1}{2}.m_3.v_3^2 + \frac{1}{2}.I_3.(\theta_2' - \theta_1')^2 \quad (12) \qquad T_4 = \frac{1}{2}.m_4.v_4^2 + \frac{1}{2}.I_4.(\theta_2' + \theta_1')^2 \quad (13)$$

The Lagrangian of the system is calculated by taking $L = T_{sum}(\theta, \theta') - U(\theta)$ and $U(\theta) = 0$. The Lagrangian of the system is given in equation (14).

$$L = \frac{1}{8}.\zeta.\theta_1'^2 + \frac{1}{8}.\eta.\theta_2'^2 + \frac{1}{8}.\varepsilon.\cos(\theta_2 - \theta_1).\theta_1'.\theta_2' + (I_4 - I_3).\theta_1'.\theta_2' \quad (14)$$

In the resulting Lagrangian, 3 parts consisting of constants are expressed as the parameters ζ, η, ε, respectively and are given in equations (15), (16), (17).

$$\zeta = 2.\left(m_1.L_1^2 + 4.I_1\right) + 4.\left(m_3.L_1^2 + I_3\right) + 4.(m_4.(L_1 + L_5/2) + I_4) \quad (15)$$

$$\eta = \left(m_2.L_2^2 + 4.I_2\right) + \left(m_3.L_2^2 + 4.I_3\right) + 4.\left(m_4.L_2^2 + I_4\right) \quad (16)$$

$$\varepsilon = 4.m_3.L_1.L_2 + 8.m_4.L_2.(L_1 + L_5/2)) \quad (17)$$

In conservative systems, Lagrange's equation of motion is given by (18) [Marion 1965].

$$\frac{\mathrm{d}}{\mathrm{dt}}\frac{\partial \mathrm{L}}{\partial(\theta_1', \theta_2')} - \frac{\partial \mathrm{L}}{\partial(\theta_1, \theta_2)} + \frac{\partial \mathrm{D}}{\partial(\theta_1', \theta_2')} = (\tau_1, \tau_2) \quad (18)$$

$\theta_1$ and $\theta_2$ are the joint angles (rad.). $\tau_1$, $\tau_2$ are torque (N.m) corresponding to the joint angles and D is dissipating energy (joules). We use Lagrange's equation to drive manipulandum dynamics.

$$\frac{\mathrm{d}}{\mathrm{dt}}\left(\frac{\partial \mathrm{L}}{\partial \theta_1'}\right) = \frac{1}{4}.\zeta.\theta_1'' - \frac{1}{8}.\varepsilon.\sin(\theta_2 - \theta_1).(\theta_2' - \theta_1').\theta_2' + \left(\frac{1}{8}.\varepsilon.\cos(\theta_2 - \theta_1) + (I_4 - I_3)\right).\theta_2'' \quad (19)$$

$$\frac{\partial \mathrm{L}}{\partial \theta_1} = \frac{1}{8}.\varepsilon.\sin(\theta_1 - \theta_2).\theta_1'.\theta_2' \quad (20)$$

$$\frac{\mathrm{d}}{\mathrm{dt}}\left(\frac{\partial \mathrm{L}}{\partial \theta_2'}\right) = \frac{1}{4}.\eta.\theta_2'' - \frac{1}{8}.\varepsilon.\sin(\theta_2 - \theta_1).(\theta_2' - \theta_1').\theta_1' + \left(\frac{1}{8}.\varepsilon.\cos(\theta_2 - \theta_1) + (I_4 - I_3)\right).\theta_1'' \quad (21)$$

$$\frac{\partial \mathrm{L}}{\partial \theta_2} = -\frac{1}{8}.\varepsilon.\sin(\theta_1 - \theta_2).\theta_1'.\theta_2' \quad (22)$$

$$\tau = M(\theta).\theta'' + V(\theta, \theta') \quad (23)$$

$M(\theta)$ and $V(\theta, \theta')$ are written in matrix form as in (24) and (25).

$$M(\theta) = \begin{bmatrix} \frac{1}{4}.\zeta & \frac{1}{8}.\varepsilon.\cos(\theta_2 - \theta_1) + (I_4 - I_3) \\ \frac{1}{8}.\varepsilon.\cos(\theta_2 - \theta_1) + (I_4 - I_3) & \frac{1}{4}.\eta \end{bmatrix}.\begin{bmatrix} \theta_1'' \\ \theta_2'' \end{bmatrix} \quad (24)$$

$$V(\theta, \theta') = \begin{bmatrix} \frac{1}{8}.\varepsilon.\sin(\theta_2 - \theta_1).(2.\theta_1' - \theta_2').\theta_2' + (C_1 + C_3 + C_4).\theta_1' + (C_4 - C_3).\theta_2' \\ \frac{1}{8}.\varepsilon.\sin(\theta_2 - \theta_1).(\theta_1' - 2.\theta_2').\theta_1' + (C_2 + C_3 + C_4).\theta_2' + (C_4 - C_3).\theta_1' \end{bmatrix} \quad (25)$$

If we leave the $\theta''$ expression alone in equation (7), we obtain the dynamic equation of the system depending on the torque and external force variables.

$$\theta'' = M(\theta)^{-1}(\,\tau - V(\theta, \theta') - \ J(\theta)^T f\,) \quad (26)$$

Before presenting the details of controller, the manipulandum 3D dynamic model created in Simulink Simscape Multibody (SSM) should also be mentioned. SSM allow the representation of all links, revolute joints, rotational and translational rigid transformations. Internal mechanic properties (stiffness, damping coefficient) are adjustable. Also, physical shape and material density of the links can be adjustable. Close chain structure, fixed frame relations, inputs and outputs of the platform can be seen on Figure-1.

### II.3. IMPEDANCE CONTROLLER

When it comes to human interaction, in addition to position control, the force applied to the end-effector should also be controlled. Impedance control; aims at the control of position and force by adjusting the mechanical impedance due to the external force applied by the person to the end-effector.

Mechanical impedance is related to the moving forces acting on a mechanical system. Mechanical impedance is defined by the rate of change of force acting on a body to the velocity generated by the same force [17],[18],[19].

In impedance control the operator motion is an input and the reaction force is fed back to the operator based on this input measurement. We also assume that the desired impedance of the body to the external force is expressed by,

$$m_d.\theta'' + D_d.(\theta' - \theta_d') + K_d.(\theta - \theta_d) = K_{fd}.f \quad (27)$$

where $m_d$, $D_d$, $K_d$ and $K_{fd}$ are the desired inertia matrix, damping, stiffness and external force coefficient respectively, and $\theta_d' = [\theta_{d1}'; \theta_{d2}']$ (rad/s) and $\theta_d = [\theta_{d1}; \theta_{d2}]$ (rad) are the desired velocity and position trajectories.

When $\theta$, $\theta'$and $\theta''$ are measurable, the control rule is that the torque is obtained by drawing it from the dynamic equation (7) and substituting it in the impedance equation (27). However, when the external force $f$ is measurable, the control rule is obtained by drawing $\theta''$ from the dynamic equation and substituting it in the impedance equation (27). Since no mass change is foreseen in the system, the original mass $M(\theta)$ is considered equal to the desired inertia matrix $m_d$. Thus, simplified position and velocity feedback control rule is achieved:

$$\tau = \frac{M(\theta)}{m_d}.D_d.(\theta_d' - \theta') + \frac{M(\theta)}{m_d}.K_p.(\theta_d - \theta) + V(\theta,\theta') + J(\theta)^T f + \frac{M(\theta)}{m_d}.K_{fd}.f \quad (28)$$

## III. SIMULATION INFORMATION

The manipulandum, whose parameters are shown in Figure-1(a) and (b), was simulated in the Matlab/Simulink environment. First of all, the compatibility of the dynamic model obtained with ELM and the SSM dynamic model described in Section II.2 was examined. The parameter set for both models is given in Table-1. The parameters chosen for both models are different. Damping coefficient was given to the revolute joints to represent the frictions in the SSM dynamic model. On the other hand, in the ELM dynamic model, frictions are represented by the calculation of dissipating energy.

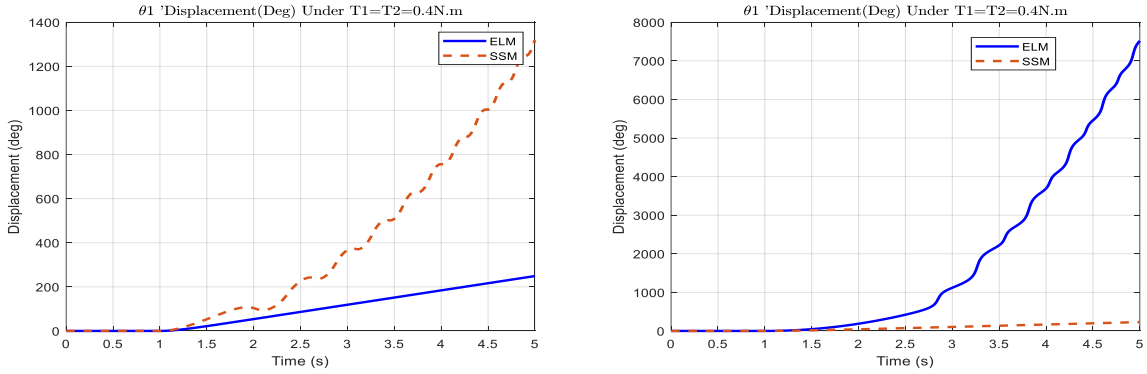


**Figure. 2.(a, b)** $[\theta_1; \theta_2]$ displacement response under $[\tau_1; \tau_2] = [0.4; 0.4]$ step input.

In Figure.2.(a), in the SSM dynamic model, the damping ratio value entered for the joints is taken as zero. In Figure.2.(b), in the ELM dynamic model, the friction coefficients "$C_i$" used in the calculation of dissipating energy are taken as zero. Both dynamic models show similar behavior in the absence of coefficients chosen to represent friction.

In the SSM dynamic model, mass moment of inertia is automatically calculated from link dimensions and link weights. However, there were difficulties in calculating the mass moment of inertia in the ELM dynamic model, especially for the end-effector. Aluminum material was chosen for the links for both models. Accordingly, density=1475 kg/m3 for half-hollow sigma profile. The center of gravity selected for L4+L5+End Effector in the ELM model may not be compatible with the SSM dynamic model. When the mass moment of inertia values used in the SSM dynamic model are applied to the ELM dynamic model, no meaningful results can be obtained (Figure.3).

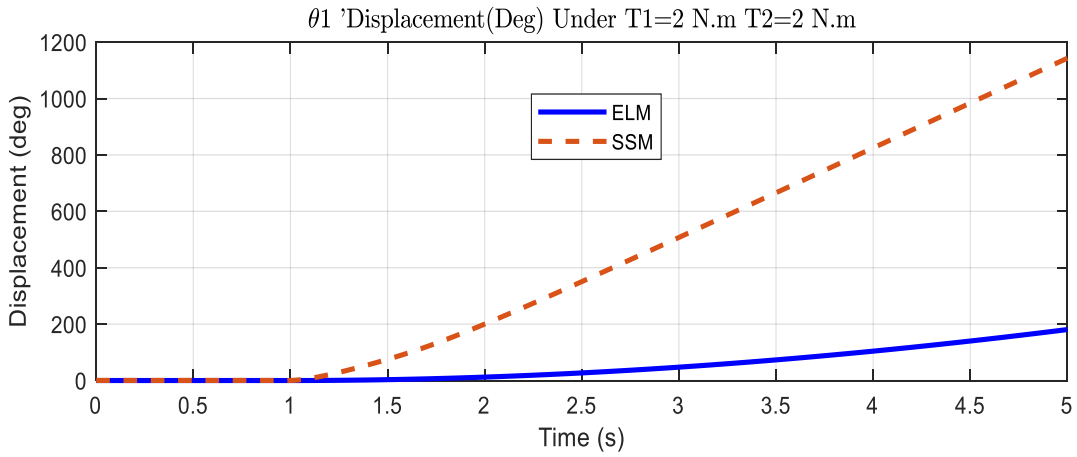


**Figure. 3.** $\theta_1$ displacement response under $[\tau_1; \tau_2] = [2; 2]$ step input.

**Table I.** Parameters for both dynamic model

| Symbol | Description | ELM Dynamic Model Value SI | SSM Dynamic Model Value SI |
|---|---|---|---|
| $L_1$=$L_3$ | Link Length | 0.20 m | 0.20 m |
| $L_2$=$L_4$ | Link Length | 0.40 m | 0.40 m |
| $L_5$ | Link Length | 0.15 m | 0.15 m |
| $m_1$ | Link Weight | 0.118 Kg | 0.118 Kg |
| $m_2$ | Link Weight | 0.236 Kg | 0.236 Kg |
| $m_3$ | Link Weight | 0.236 Kg | 0.236 Kg |
| $m_4$ | Link + End-effector Weight | 0.506 Kg | 0.506 Kg |
| $p_{1,2,3,4}$ | Center of Mass point | Undefined | Undefined |
| $I_1$ | Mass Moment of inertia of $L_1$ | 0.1 Kg.m$^2$ | 0.8*10$^{-5}$ Kg.m$^2$ |
| $I_2$ | Mass Moment of inertia of $L_2$ | 0.5 Kg.m$^2$ | 1.6*10$^{-5}$ Kg.m$^2$ |
| $I_3$ | Mass Moment of inertia of $L_3$ | 0.5 Kg.m$^2$ | 1.6*10$^{-5}$ Kg.m$^2$ |
| $I_4$ | Mass Moment of inertia of $L_4$ +$L_5$ +End-effector | 8 Kg.m$^2$ | 8.4*10$^{-5}$ Kg.m$^2$ |
| $C_1$ | Friction Coefficient $L_1$ | 0.09 N.s/m | Undefined |
| $C_2$ | Friction Coefficient $L_2$ | 0.09 N.s/m | Undefined |
| $C_3$ | Friction Coefficient $L_3$ | 0.09 N.s/m | Undefined |
| $C_4$ | Friction Coefficient $L_4$ +$L_5$ +End-effector | 0.13 N.s/m | Undefined |
| $\zeta_1$ | Damping ratio for $L_1$ | Undefined | 0.36 N.m/(rad/s) |
| $\zeta_2$ | Damping ratio for $L_2$ | Undefined | 0.36 N.m/(rad/s) |
| $\zeta_3$ | Damping ratio for $L_3$ | Undefined | 0.036 N.m/(rad/s) |
| $\zeta_4$ | Damping ratio for $L_4$ +$L_5$ +End-effector | Undefined | 0.036 N.m/(rad/s) |

Both dynamic models are compared under two basic cases. In the first case, the torque step input value was entered at t=1s to represent the actuators connected to the manipulandum $L_1$ and $L_2$ active links, and the outputs are evaluated below.

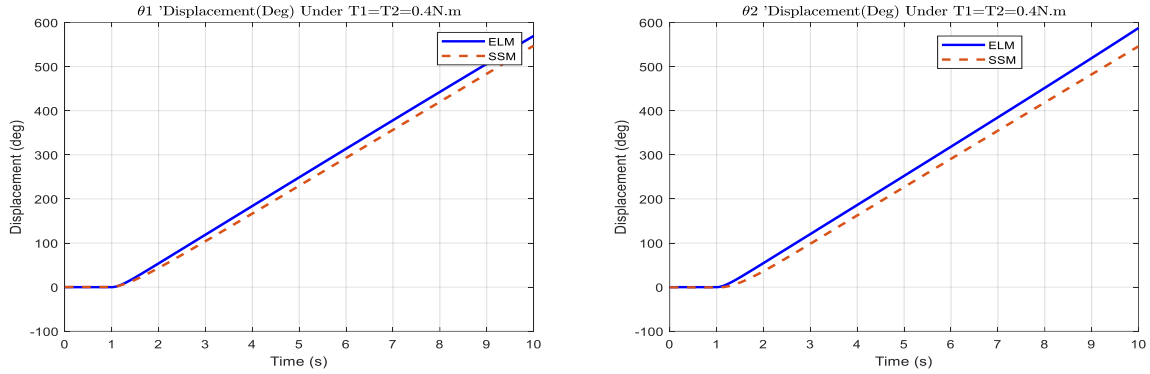


**Figure. 4.(a, b)** $[\theta_1; \theta_2]$ displacement response under $[\tau_1; \tau_2] = [0.4; 0.4]$ step input.

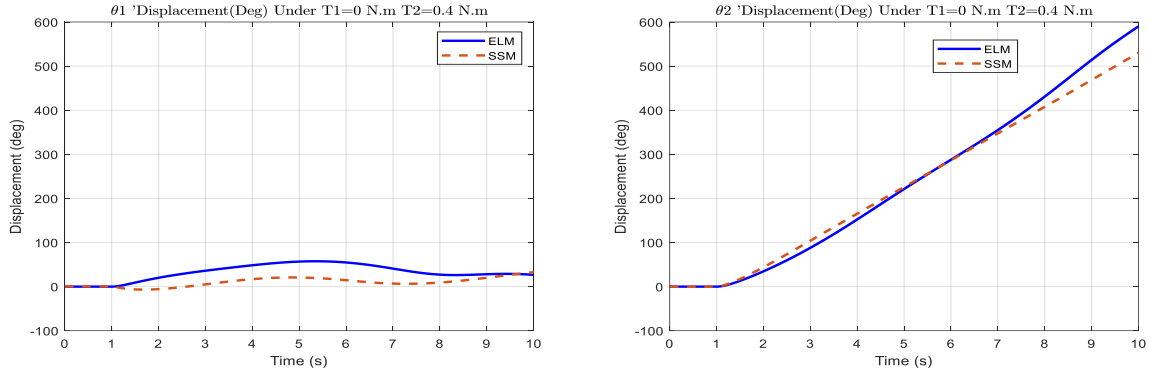


**Figure. 5.(a, b)** $[\theta_1; \theta_2]$ displacement response under $[\tau_1; \tau_2] = [0; 0.4]$ step input.

In accordance with the entered $\tau_1$ and $\tau_2$ torque input values, it is seen that $\theta_1$ and $\theta_2$ values increase in the same direction for both dynamic models during the simulation period (Figure.4. a, b). If the torque step input value entered for relevant actuator is zero, the connected link is not expected to move. However, as seen in figure.5.a, although the torque value entered for $L_1$ is zero, movement is observed in $\theta_1$. These movements can be explained by the effect of the friction defined in the joints on other motionless links. In the second case, the force $(f_x, f_y)$ step input value was entered at t=1s to represent the effect of the person's hand on the manipulandum end-effector, and the outputs are displayed below.

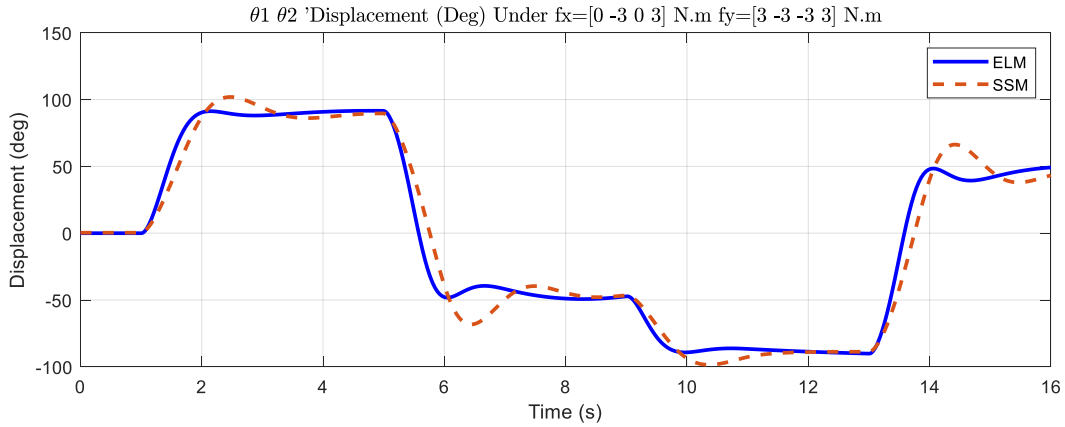


**Figure. 6.** $[\theta_1; \theta_2]$ displacement response under $[f_x] = [0 - 3\ 0\ 3]$, $[f_y] = [3 - 3 - 3\ 3]$ step input.

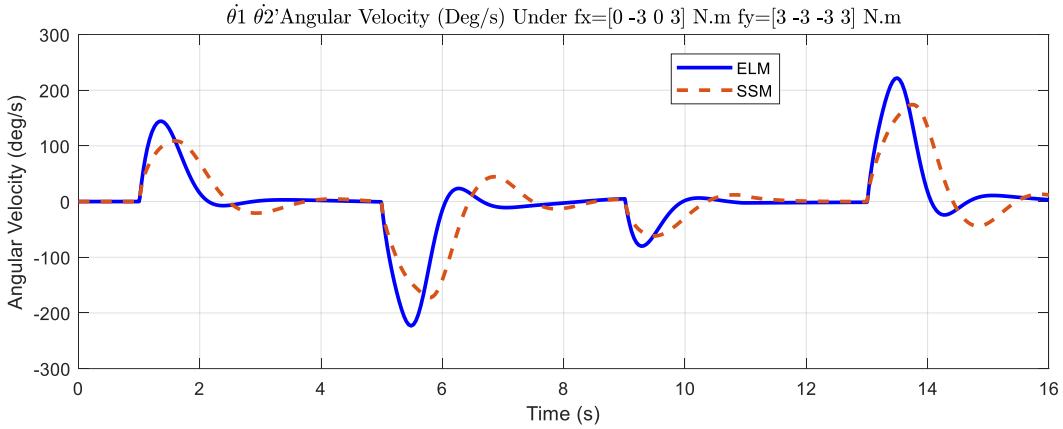


**Figure. 7.** $[\theta_1'; \theta_2']$ angular velocity response under $[f_x] = [0 - 3\ 0\ 3]$, $[f_y] = [3 - 3 - 3\ 3]$ step input.

In order to understand the effect of the step input force entered into the end-effector, a force of 3 Nm. was applied in different directions at different times t. The expectation is that the end-effector will position itself with the longest reach in the direction in which the force is entered. The system shows acceptable overshoot but behaves as expected.

After this evaluation of the dynamic model, controller simulation was started. The impedance controller explained in Section II.3 was tried to be applied to both dynamic models under the same conditions and with the same control coefficients. Kd, Dd and Kfd coefficients were determined by trial-and-error method.

First, the relationship between actuator torque input and end-effector force input was examined with the simulation. The expectation is that the extremely high selected input value will dominate the other (Figure.8.a.b).

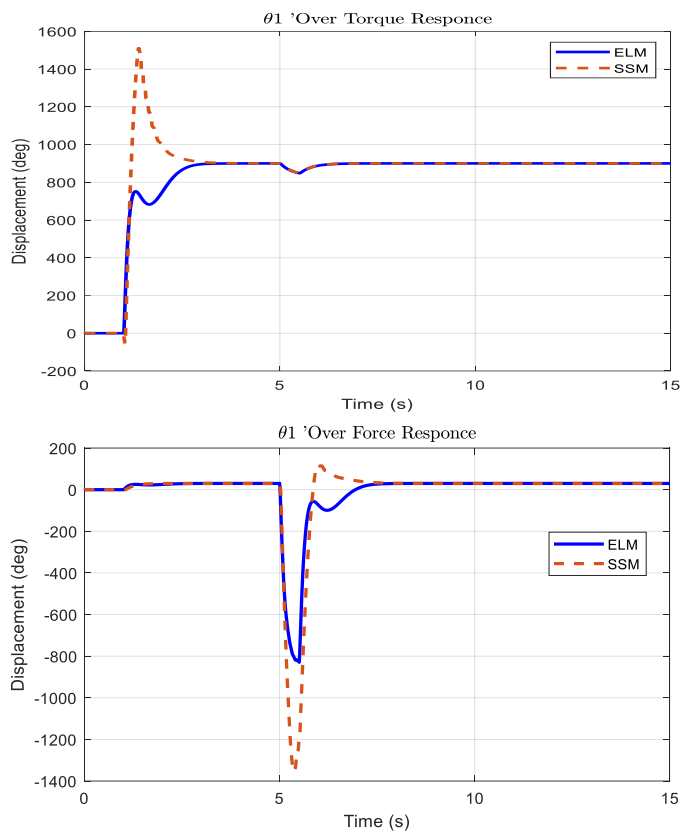


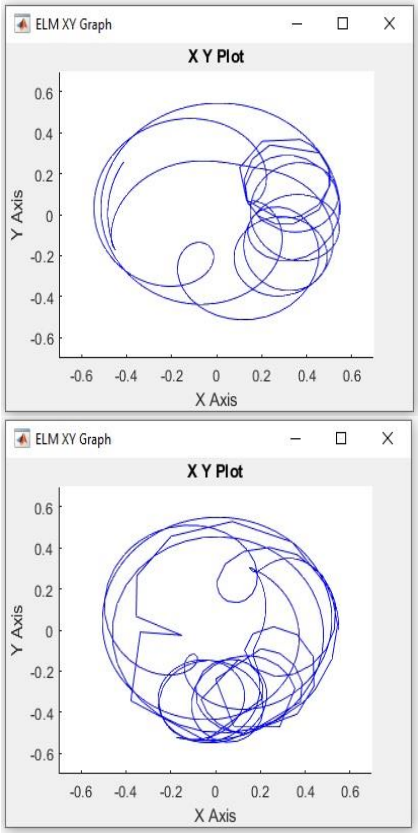


**Figure. 8.(a)** Over torque and over force responses.

**Figure. 8.(b)** XY Graphs for left site

As expected, a small Dd dumping coefficient caused the system to be under-damped, while a high Dd dumping coefficient caused the system to be over-dumped (Figure.9).

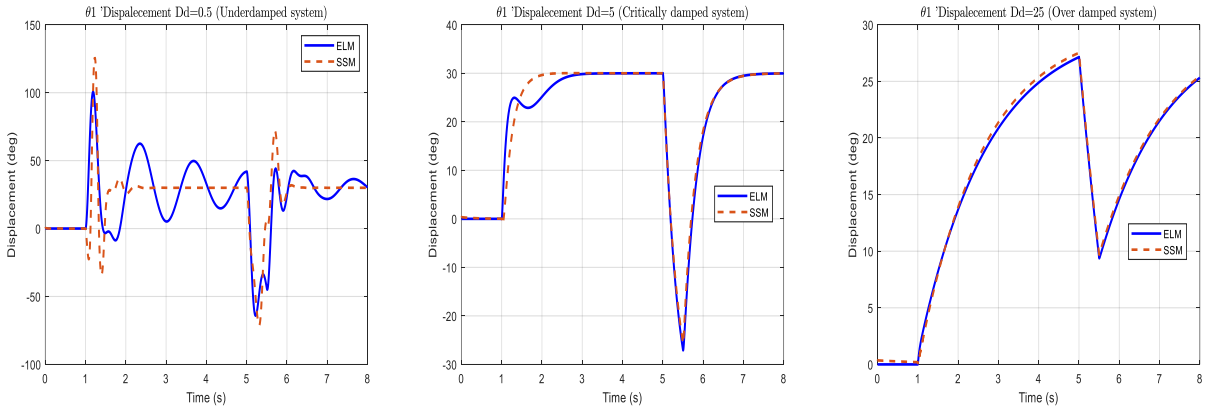


**Figure. 9** $\theta_1 = 30^o$ displacement response under damping coefficient $D_d$=0.5, $D_d$=5, $D_d$=25

Again, while a small $K_d$ stiffness coefficient caused the system to be over-dumped, a high $K_d$ stiffness coefficient caused the system to be under-dumped (Figure.10).

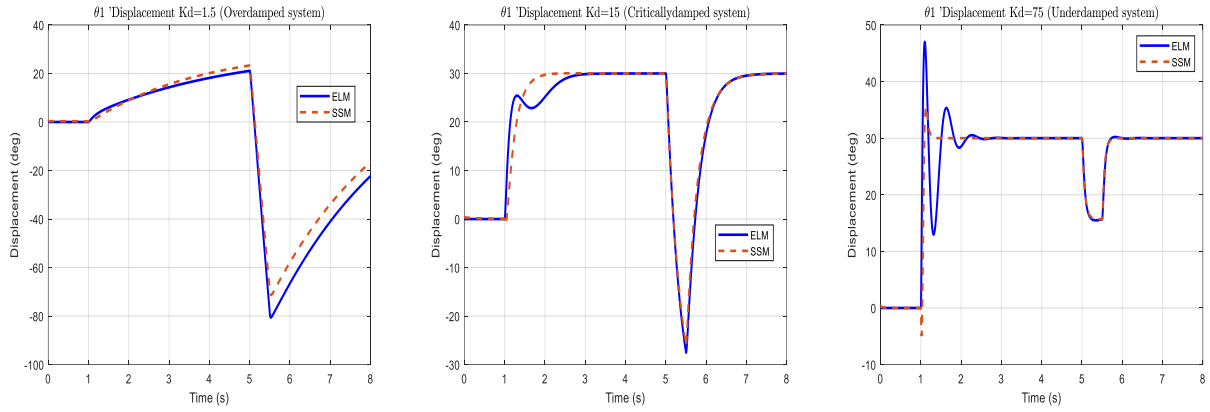


**Figure. 10** $\theta_1 = 30^o$ displacement response under stiffness coefficient $K_d$=1.5, $K_d$=15, $K_d$=75

Then, external force coefficients were tested with Kfd = (0.7, 7, 70) while the coefficients Dd = 4.89 and Kd = 14.92 were kept constant at their ideal values. It was observed that the force changed scalar in direct proportion to the change in the Kfd coefficient, but there was no deformation in the movement profile. Here $F_{xy}$ force value and is accepted as the value read by the force sensors located in the manipulandum end-effector. $[\theta_1; \theta_2] = [30^o; 140^o]$ step input was applied to the system at time $t = [5; 7.5; 10; 12.5]$ (s), during Dt=0.5 s, in ±X and ±Y directions, and the results are shared in figure.11.

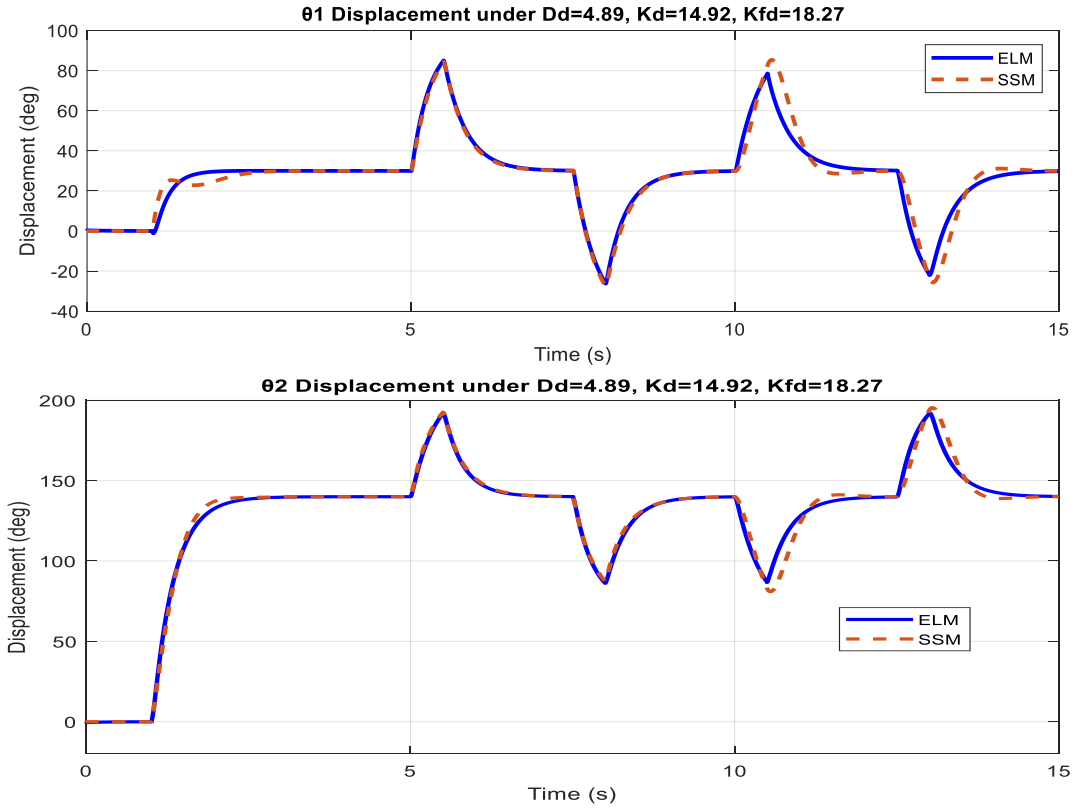


**Figure. 11** $[\theta_1; \theta_2] = [30^o; 140^o]$ displacement during applied external force on ±X and ±Y directions

## IV. DISCUSSION AND CONCLUSION

This study explains the dynamic solution of the manipulandum that interact with the human upper arm, controller design, model simulation and simulation results. Manipulandum design in this field are used in human-machine interaction experiments to understand human motor learning skills. While the subject of experiments is handled in the field of medicine, appropriate manipulandum design is the subject of the engineering field. In this study, the engineering qualities of the device were evaluated, its mathematical model obtained, dynamic model simulation done and control elements were examined. The manipulandum have a 2-dof, 5-link closed chain structure that moves in the horizontal plane, their movement is provided by 2 actuators, their interaction with the human upper arm is made with a fixed joystick (end-effector) on the 2nd link, their dimensions are smooth and compatible with the human upper arm. It is understood that the manipulandum must be of a size that can safely interact with the human arm. A conceptual design was made for the manipulandum and the movement parameters of the manipulandum were obtained by creating a kinematic model accordingly. While creating the dynamic model of the system; It is accepted that the manipulandum moves in the horizontal plane, therefore there is no effect of gravity, there is no spring, damper or similar potential energy source in the system, and there is heat loss due to friction. The dynamic model obtained with the ELM was compared with the system model obtained with the SSM tool in the Simulink environment; The consistency of model parameters (friction coefficients, moment of inertia, etc.) was mutually checked. Since human-manipulandum interaction requires force control, an impedance controller has been designed for the system dynamics, instead of classical controllers. The success of the controller on both the ELM dynamic model and the model created in SSM was examined and the results were evaluated.

Result of the simulations suggests that in order to achieve meaningful position and force control, there must be a proportional magnitude relationship between the torques applied to the model by the actuators and the force applied to the end-effector. If the actuator torques or end-effector forces are excessively greater than the other, the simulation results in two ways. In cases where the force is dominant, the manipulandum moves in unpredictable / unexpected trajectories around the origin. In the case where the torque is dominant, the manipulandum rotates around the origin until the end of the simulation period and its rotation is in the direction where the torque is dominant. This is an expected situation. Human-machine interaction safety and effectiveness are also mention in similar articles reviewed.

**Future work:** In this study, no working condition or working area restrictions were defined for the manipulandum. However, in a Manipulandum prototype it should be ensured that the links do not pass over each other (up & down link relationship). Links should be prevented from falling into cross positions. System workspace (boundary) must be defined. The system must be prevented from making a full rotation (360-degree rotation). This study was supported by Kafka Mechatronics Co. With this support, the manipulandum prototype was completed and the electronic components and software infrastructure for the actuators, drivers and controller were prepared. The results obtained from the experimental setup will also be shared in an article, and the entire study will be converted into a doctoral thesis and shared.

### STATEMENT OF CONTRIBUTION RATE

Authors' contribution rates to the study are equal.

### CONFLICTS OF INTEREST

They reported that there was no conflict of interest between the authors and their respective institutions.

### RESEARCH AND PUBLICATION ETHICS

In the studies carried out within the scope of this article, the rules of research and publication ethics were followed.

## REFERENCES

[1] A. (Lex) E. Q. vanDelden, C. (Lieke) E. Peper, Gert Kwakkel, and Peter J. Beek, "A Systematic Review of Bilateral Upper Limb Training Devices for Poststroke Rehabilitation", Hindawi Publishing Corporation Stroke Research and Treatment, Volume 2012, Article ID 972069, 17 pages doi:10.1155/2012/972069

[2] Ian S. Howard, James N. Ingram, David W. Franklin, * and Daniel M. Wolpert*, "Gone in 0.6 Seconds: The Encoding of Motor Memories Depends on Recent Sensorimotor States", The Journal of Neuroscience, September 12, 2012, 32(37):12756 –12768

[3] Ian S. Howard, Christopher Ford, Angelo Cangelosi & David W. Franklin, "Active lead-in variability affects motor memory formation and slows motor learning", http://www.nature.com/scientificreports, August 10, 2017

[4] Hiroaki Gomi, Mitsuo Kawato, "Human arm stiffness and equilibrium-point trajectory during multi-joint movement", Biological Cybernetics, Biol. Cybern.76, 163-171 (1997)

[5] BKIN Technologies Ltd. dba Kinarm., "Kinarm Tech End Point Lab", PN14332-1-Nov-21, www.kinarm.com (accessed 24th May 2024)

[6] Klein J., Roach N., and Burdet E., "3DOM: A 3 Degree of Freedom Manipulandum to Investigate Redundant Motor Control", IEEE Transactions On Haptics, Vol.7 No.2 April-June 2014

[7] Kostic M. D., Popovic M. B., "Influence of Planar Manipulandum to the Hand Trajectory During Point to Point Movement", IEEE International Conference on Rehabilitation Robotics, ETH Zurich City, Switzerland, 2011

[8] Fong J., Crocher V., Tan Y., Oetomo D., and Mareels I., "EMU: A Transparent 3D Robotic Manipulandum for Upper-limb Rehabilitation", International Conference on Rehabilitation Robotics (ICORR), QEII Centre, London, UK, July 17-20, 2017

[9] Ueyama Y., and Miyashita E., "Optimal Feedback Control for Predicting Dynamic Stiffness During Arm Movement", IEEE Transactions on Industrial Electronics, Vol. 61, No.2, February 2014

[10] Cai S., Wu W., and Xie L., "Dual-Arm Limb Rehabilitation Robot: Mechanism Design and Preliminary Experiments", 6th International Conference on Control, Automation and Robotics, 2020

[11] Nguyen K. T., and Nguyen H. D., "Designing the Robot Arms for Upper Limb Recovery Movements of Post-Stroke Patients", 6th International Conference on Green Technology and Sustainable Development (GTSD), 2022

[12] Asgari M., and Crouch D. L., "Estimating Human Upper Limb Impedance Parameters From a State-of-the-Art Computational Neuromusculoskeletal Model", 43rd Annual International Conference of the IEEE Engineering in Medicine & Biology Society (EMBC), Virtual Conference, Oct. 21 – Nov. 4, 2021

[13] Erwin de Vlugt, Alfred C. Schouten, Frans C.T. van der Helm, Piet C. Teerhuis, Guido G. Brouwn, "A force-controlled planar haptic device for movement control analysis of the human arm", Journal of Neuroscience Methods 129 (2003) 151-168

[14] John J. Craig, "Introduction to Robotics Mechanics and Control", Pearson Education 2018, Fourth Edition, Global Edition, ISBN 978-0-13-348979-8

[15] F. C. Park and K. M. Lynch, "Introduction to Robotics Mechanics, Planning, and Control", Park and Lynch 16:36 September 20, 2016

[16] Mark W. Spong, Seth Hutchinson, and M. Vidyasagar, "Robot Dynamics and Control" Second Edition, January 28, 2004

[17] Frank L.Lewis, Darren M.Dawson, Chaouki T.Abdallah, "Robot Manipulator Control Theory and Practice", Second Edition, Revised and Expanded Copyright © 2004 by Marcel Dekker, Inc.

[18] Bruno Siciliano, Lorenzo Sciavicco, Luigi Villani, Giuseppe Oriolo, "Robotics Modelling, Planning and Control", Springer-Verlag London Limited, 2009, DOI 10.1007/978-1-84628-642-1

[19] Asif SŠabanovic, Kouhei Ohnishi., "Motion Control Systems", First Edition, Published 2011 by John Wiley & Sons (Asia) Pte Ltd. ISBN: 978-0-470-82573-0